Bark beetle controls epithelial morphogenesis by septate junction maturation in *Drosophila*

Anja Hildebrandt [a], Ralf Pflanz [b], Matthias Behr [d], Theresa Tarp [a], Dietmar Riedel [c], Reinhard Schuh [a,*]

[a] Research Group Molecular Organogenesis, Germany
[b] Department of Molecular Developmental Biology, Germany
[c] Electron Microscopy Group, Max-Planck-Institute for Biophysical Chemistry, Am Fassberg, D-37077 Göttingen, Germany
[d] Developmental Biology, University of Leipzig, Talstrasse 33, D-04103 Leipzig, Germany

ARTICLE INFO

ABSTRACT

Epithelial tissues separate body compartments with different compositions. Tight junctions (TJs) in vertebrates and septate junctions (SJs) in invertebrates control the paracellular flow of molecules between these compartments. This epithelial barrier function of TJs and SJs must be stably maintained in tissue morphogenesis during cell proliferation and cell movement. Here, we show that Bark beetle (Bark), a putative transmembrane scavenger receptor-like protein, is essential for the maturation but not the establishment of SJs in *Drosophila*. Embryos that lack *bark* establish functional SJs, but due to rudimentary septae formation during subsequent embryonic development, these become non-functional. Furthermore, cell adhesion is impaired at the lateral cell membrane and the core protein complexes of SJs are mis-localised, but appear to form otherwise normally in such embryos. We propose a model in which Bark acts as a scaffold protein that mediates cell adhesion and mounting of SJ core complexes during cell rearrangement in tissue morphogenesis.

© 2015 Elsevier Inc. All rights reserved.

Introduction

Epithelial sheets control the transepithelial flow of ions and solutes crucial for homoeostasis within various body compartments (Rodriguez-Boulan and Nelson, 1989). The molecular basis of this transepithelial barrier function is comprised of multi-protein complexes localised in the lateral cell membrane of epithelial cells, the tight junctions (TJs) in vertebrates and septate junctions (SJs) in invertebrates (Schneeberger and Lynch, 1992; Tepass et al., 2001; Tsukita et al., 2001).

The morphological and functional key components of TJs are claudins, integral membrane proteins with four transmembrane-spanning regions (Turksen and Troy, 2004). The claudin family consists of 24 members in mice and humans. They show distinct tissue-specific expression patterns and interact *via* homo- and/or heterophilic binding (Angelow et al., 2008; Lal-Nag and Morin, 2009). It is assumed that the combination and proportion of claudins contribute to the distinct barrier specificities in various tissues (Tsukita and Furuse, 2002).

Claudins are also integral parts of the invertebrate SJs, the functional homologues of TJs (Furuse and Tsukita, 2006). The *Drosophila* SJs contain three claudins, Kune kune (Kune; Nelson et al., 2010), Sinuous (Sinu; Wu et al., 2004) and Megatrachea (Mega; Behr et al., 2003). The claudin Mega shows interaction with the integral SJ transmembrane component Neurexin IV (NrxIV, Baumgartner et al., 1996) and the intracellular scaffolding SJ component Coracle (Cora; Lamb et al., 1998) by genetic evidence (Behr et al., 2003). Furthermore, the SJ proteins reveal a high degree of physical interaction, e.g. pull down assays show specific binding between the Varicose (Vari) PDZ-domain and the NrxIV C-terminus (Wu et al., 2007), and Cora and NrxIV interact directly *via* the amino-terminal region of Cora and the cytoplasmic tail of NrxIV (Ward et al., 1998). In addition, analysis of the Mega interactom using immunoprecipitation and mass spectrometry identified nine established SJ components associated with Mega (Jaspers et al., 2012).

Recent results from fluorescent recovery after photobleaching (FRAP) experiments suggest that SJs are composed of a single, highly ordered multiprotein complex, the SJ core complex (Oshima and Fehon, 2011), which consists of at least the Na^+/K^+-ATPase $\tilde{\alpha}$ and $\tilde{\beta}$ subunits (Genova and Fehon, 2003; Paul et al., 2003), Cora, Mega, Neuroglian (Nrg; Genova and Fehon, 2003), NrxIV, Sinu and Vari. It was proposed, that these core proteins assemble into

intracellular complexes which slowly move and finally locate to the SJs (Oshima and Fehon, 2011). Loss- and gain-of function mutations in any of these core SJ components cause the mis-localisation of the other SJ proteins indicating a high degree of interdependence. In addition, the structure and function of SJs is impaired in such mutants (Behr et al., 2003; Nelson et al., 2010).

Normal SJs are characterised by the ladder-like structure in electron microscopic pictures with septae (steps) connecting plasma membranes across the intercellular space of adjacent epithelial cells (Knust and Bossinger, 2002; Tepass et al., 2001). In mutants of SJ components the septae and the ladder-like structure are disrupted. Furthermore, in such mutants the transepithelial barrier function is compromised as revealed by dye injection experiments (Behr et al., 2003; Lamb et al., 1998; Ward et al., 2001). SJs are also required for the apical secretion of the luminal matrix modifying enzymes, Serpentine (Serp) and Vermiform (Verm) in the developing tracheal system. This secretory pathway is specific for Verm and Serp, since other apical proteins are normally secreted in SJ mutants (Luschnig et al., 2006; Wang et al., 2006).

During epithelial tissue morphogenesis cells need to extensively rearrange as a result of proliferation and cell movement. While cells reshuffle SJs must maintain the transepithelial barrier function to ensure homoeostasis. A model of epithelial cell rearrangement has been proposed in which septae are redistributed while the transepithelial barrier is maintained without requiring rapid breakdown and rebuilding of SJ components (Fristrom, 1982). However, not much is known about the molecular mechanisms and the molecules that are involved in SJ maturation and reshuffling.

Here we describe the identification and functional characterisation of the putative scavenger receptor-like protein Bark beetle (Bark; CG3921), which was previously identified as an interaction partner of the claudin Mega (Jaspers et al., 2012). Bark is required for SJ maturation in developing epithelial cells. We also provide evidence that Bark controls epithelial cell adhesion within the SJ compartment. In bark mutants the SJ core complexes are normally assembled but become mis-localised during epithelial differentiation. We propose that Bark binds SJ core protein complexes via Mega to establish functional SJs during the reshuffling process of SJ components.

Materials and methods

Immunochemistry

Anti-Bark antibodies against peptides EGYEQKPHYNEYVNQN (amino acids 78–93) and PEYQRSSHSSFMPHRSSGD (amino acids 220–238) were generated in guinea pig by PSL GmbH (Heidelberg, Germany) and used in a 1:500 dilution. Anti-Kune antibodies against peptides ISEYGDEYYQNQGPSC (amino acids 208–223) and ESRPRRP-QQSSASNSA (amino acids 239–255) were generated in rabbit by Eurogentec (Cologne, Germany) and used in a 1:50 dilution. Additional antibodies were used as follows: anti-Mega (1:20; Jaspers et al., 2012), anti-Verm (1:100) and anti-Serp (1:200; Luschnig et al., 2006, gift from S. Luschnig), anti-Crb (1:250; Cq4, Tepass et al., 1990), anti-FasIII (1:500; 7G10, Patel et al., 1987), anti-Ecad (1:20; DCAD2, Oda et al., 1994), anti-Phosphotyrosine (1:500; PY20, Enzo Life Science), anti-Cora (1:500; C566.9, Fehon et al., 1994), anti-Dlg (1:20; 4F3, Parnas et al., 2001) anti-Chc (1:40; Wingen et al., 2009), anti-Rab5 (1:30; Wucherpfennig et al., 2003), Rab7 (1:100; Chinchore et al., 2009), anti-Rab11 (1:250; Satoh et al., 2005), anti-Lamp1 (1:100; Rusten et al., 2006) and anti-GFP (1:500; Abcam). If not indicated otherwise, primary antibodies were obtained from the Developmental Studies Hybridoma Bank (DSHB). The following secondary antibodies were used in 1:500 dilutions:goat anti-mouse IgG Alexa568, goat anti-mouse IgG Alexa488, goat anti-guinea pig IgG Alexa488, goat anti-rabbit IgG Alexa568, goat anti-rabbit IgG Alexa488 (Invitrogen) and goat anti-chicken Alexa488 (Jackson ImmunoResearch). Fluorescein-conjugated chitin-binding probe (NEB) was used in a 1:500 dilution to stain the tracheal lumen. Image acquisitions were performed with a LSM710 or a LSM780 confocal microscope (Zeiss) and a LD LCI Plan-Apochromat $25 \times$ /0.8 Imm Corr DIC M27 or a Plan-Apochromat $40 \times$ /1.4 Oil DIC M27 oil immersion or a $63 \times$ /1.3 Imm Corr DIC M27 LCI Plan-Neofluar (water) objective using standard settings.

Dextran red permeability experiments

bark[23H]/Df(2L)BSC171 embryos were identified by the lack of the CyO, P{w[+mC]=Dfd-eYFP} balancer chromosome (Le et al., 2006). Dechorionated embryos at stage 17 were covered with Voltalev 10S oil for injection. Rhodamine-labelled dextran (MW 10,000; Molecular Probes) was purified and injected into the haemocoel of embryos as described previously (Lamb et al., 1998). The embryos were immediately analysed by confocal microscopy.

Electron microscopy and chitin labelling

Living stage 15, 16 and 17 Drosophila embryos were mechanically dechorionated and placed on a 150 μm flat embedding specimen holder (Engineering Office M. Wohlwend GmbH, Sennwald, Switzerland) and frozen in a Leica HBM 100 high pressure freezer (Leica Microsystems, Wetzlar, Germany). The embedding of the vitrified samples was performed using an Automatic Freeze Substitution Unit (AFS; Leica Microsystems, Wetzlar, Germany). Substitution was done at -90 °C in a solution containing anhydrous acetone, 0.1% tannic acid and 0.5% glutharaldehyd for 72 h and in anhydrous acetone, 2% OsO4, 0.5% glutharaldehyd for additional 8 h. After a further incubation for 18 h at -20 °C samples were warmed up to $+4$ °C and subsequently washed with anhydrous acetone. The samples were embedded at room temperature in Agar 100 (Epon 812 equivalent) and polymerised at 60 °C for 24 h. Ultrathin sections were counterstained using 1% uranylacetate in methanol. Images were taken in a Philips CM120 electron microscope (Philips Inc.) using a TemCam 224 A slow scan CCD camera (TVIPS, Gauting, Germany).

Chitin was indirectly labelled using wheat germ agglutinin detection as described (Moussian et al., 2006) with the exception that the ultrathin sections of Epon embedded Drosophila embryos were incubated with 5 μg/ml biotinylated wheat germ agglutinin (Vector Labs, Burlingame, USA) followed by 1:20000 diluted rabbit anti-biotin antibodies (Rockland Inc. USA) and 10 nm protein A gold conjugates (Dr. George Posthuma, University Medical Center Utrecht, The Netherlands). Labelled sections were not counterstained for a better visibility of the gold labelling and visualised in a Philips CM120 electron microscope (Philips Inc.).

FRAP live imaging and image analysis

Dechorionated embryos at stage 16 were mounted on glass bottom microwell dishes (MatTek) and covered with PBS and coverslips. Observation and photobleaching were performed with a LSM780 confocal microscope and the Zen acquisition software (Zeiss) and a $63 \times$ /1.3 LCI Plan-Neofluar objective. GFP was photobleached with 100% output of 405 nm and 50% output of 488 nm laser for 147.58 μs/pixel. Fluorescence recovery was analysed by measuring the mean grey value at the plasma membrane of bleached areas with ImageJ (National Institutes of Health) and calculations were done with Microsoft Excel.

Fly stocks

The fly strains P{SUPor-P}KG10579, P{SUPor-P}KG01131, ATPα-GFP (ZCL1792), NrxIV-GFP (CA06597), Nrg-GFP (G305), mega[G0012], sinu[06524]

and *vari^03953b* were obtained from Bloomington Stock Center. We used the lethal P-Element insertion line P{SUPor-P}KG10579 and the viable P-Element insertion line P{SUPor-P}KG01131 for P-element jump-out experiments (Hartenstein and Jan, 1992). The generated DNA deletions of *bark^23H* and *bark^27L* were analysed by PCR amplification of genomic DNA followed by DNA sequencing of the amplicons. All mutant fly strains were balanced with a marked balancer chromosome mediating YFP fluorescence to identify homozygous embryos (Le et al., 2006). For the UAS-*bark* fly strain, the *bark* gene was cloned into the *pUAST* vector using the gene-specific primers 5′-TAGCATGAAGCTGCAACATCATAAAACCAACAG-3′ and 5′-ACTTCACATGGCCGTTTCCAGG-3′ (both with attached *NotI* restriction sites) and the transgene constructs were used for P-element-mediated germline transformation (Rubin and Spradling, 1982).

Results

bark beetle is essential for the morphogenesis and gas filling of the tracheal tubes

We recently identified the gene product of *CG3921* as a putative interactor of the claudin Mega. RNAi-mediated tracheal knock-down of *CG3921* revealed tracheal phenotypes reminiscent of mutant phenotypes affecting SJs, e.g. *mega* mutants, suggesting a role of *CG3921* in SJ formation (Jaspers et al., 2012). To generate lethal P-element jump-out *CG3921* mutants we used the P-element insertion lines P{SUPor-P}KG01131 and P{SUPor-P}KG10579. Both insertions reside in non-coding DNA-regions of CG3921 (Fig. 1A). The excision lines 27L(KG01131) and 23H(KG10579) failed to complement each other as well as the deficiency Df(2L)BSC171, which deletes the chromosomal region 24C1-6 including *CG3921*. In contrast to wild-type embryos, which show a gas filled tracheal system and straight shaped tracheal branches (Fig. 1 B and D), mutant embryos of both P-element jump-out lines do not perform liquid clearance (LC) of the tracheal tubes and reveal convoluted tracheal branches in both homozygous and hemizygous conditions over the Df(2L)BSC171 (Fig. 1C and E, not shown). Since the tracheal phenotype of the mutants resembles the tracks of bark beetle larvae we named the mutant *bark beetle* (*bark*) and the alleles *bark^27L* and *bark^23H*. The alleles were molecularly characterised as having DNA deletions in *CG3921* (Fig. 1A). In *bark^27L* and *bark^23H* the 5′-coding regions of *CG3921* are deleted (Fig. 1A) and both alleles lack any detectable *CG3921* expression (not shown). Thus, *bark^27L* and *bark^23H* represent lack-of-function *bark* alleles. Ectopic expression of the *CG3921* coding region using the UAS/Gal4 system (see Materials and methods) in the tracheal system of *bark^23H* mutant embryos by the UAS/Gal4 system (Brand and Perrimon, 1993) reveals normal gas filling of the trachea (Fig. 1F) and wild-type like tracheal morphology (Fig. 1G). Thus, these tissue-specific rescue experiments indicate that *CG3921* encodes the *bark* gene.

The transepithelial barrier is affected in bark beetle mutant embryos

Bark interacts with the SJ protein Mega (Jaspers et al., 2012) and the *bark* mutant tracheal phenotype is reminiscent of SJ mutant phenotypes. These observations suggest that functions of SJs are affected in *bark* mutant embryos. Thus, we analysed a rhodamine-labelled 10 kDa dextran for its ability to cross the transepithelial barrier by injecting the dye into the haemocoel of stage 17 embryos (Lamb et al., 1998; Ward et al., 2001). Rhodamine-dextran injections into wild-type embryos show no diffusion of the dye into the lumen of the tracheal system (Fig. 1H) as expected for a functional barrier established by the SJ in the tracheal epithelium. In contrast, red-dextran dye diffuses into the tracheal lumen of *bark* mutant embryos (Fig. 1H') indicating a damaged tracheal barrier function

typical of embryos mutant for SJ components. SJs are also essential for the exocytosis of the chitin modifying enzymes Serpentine and Vermiform (Luschnig et al., 2006; Wang et al., 2006). Interestingly, Serp and Verm are localised in the tracheal lumen of *bark* mutant embryos (Fig. 1I' and J') indicating exocytosis of these enzymes as found in wild-type embryos (Fig. 1I and J). These results, therefore, show that *bark* is essential for the main function of SJs, i.e. the transepithelial barrier, but it is not involved in the specific exocytosis processes mediated by SJs.

bark beetle is expressed in epithelial tissues and the protein localises at the lateral cell membrane

We performed in situ hybridisation on whole mount embryos to visualise *bark* transcript expression during embryonic development. A maternally contributed *bark* transcript was not detected. First zygotic *bark* transcripts arise during stage 13 in the tracheal system, the foregut, the hindgut, the salivary glands and the epidermis. The expression persists in the corresponding tissues until the end of embryogenesis (Supplementary Fig. 1). Thus, *bark* transcripts are restricted to ectodermally derived tissues during embryogenesis.

The *bark* gene encodes a putative 3123 amino acid large member of the scavenger receptor protein family with a single predicted transmembrane domain (Fig. 1K). To analyse Bark protein distribution we produced an antibody against Bark (see Materials and methods). Bark protein expression coincides with *bark* RNA pattern. A maternal contribution is not detected and first zygotic Bark protein expression starts in stage 13, while embryos deficient for *bark* show no specific staining (not shown).

The subcellular Bark distribution reveals close association with the apicolateral membrane region of hindgut epithelial cells (Fig. 2A). Cells mutant for *bark* lack any detectable staining (Fig. 2B), but show phosphotyrosine control staining (Fig. 2B' and B″). Co-immunofluorescence stainings of Bark and the SJ-marker Mega (Behr et al., 2003) show overlapping staining (Fig. 2A″), indicating Bark localisation to the SJs. Furthermore, no localisation to specific junctional regions, such as tricellular SJ, were observed. However, Bark staining is not restricted to the SJs, since it also overlaps with the adherens junction marker E-cadherin (Fig. 2C″; Oda et al., 1994). In contrast, Bark does not co-localise with Crumbs (Tepass et al., 1990), which defines the apical most membrane compartment of epithelial cells, the marginal zone (Fig. 2D″). Thus, Bark is localised in cell compartments, which form SJs and adherens junctions.

Bark beetle is essential for the proper localisation of SJ core components during late embryogenesis

Bark is localised in the region of SJ formation and it plays a role in the functional properties of SJs. Therefore, we analysed the distribution of SJ components in *bark* mutant embryos during different developmental stages. During early steps of SJ formation at stage 15 the SJ components Mega, Kune, NrxIV, Nrg and Discs large (Dlg; Woods et al., 1996) are localised in the apico-lateral cell membrane of *bark* mutant hindgut cells as found in wild-type embryos (Fig. 3A E; stage 15). These findings suggest that *bark* is not involved in the initial organisation of integral SJ components. However, Mega, Kune, NrxIV and Nrg are mis-localised at the baso-lateral membrane at stage 17 (Fig. 3A–D; stage 17), while Dlg localisation resembles wild-type (Fig. 3E; stage 17). Corresponding results of SJ marker localisation were obtained in *bark* mutant epidermal cells (Supplementary Fig. 2). This suggests that *bark* is essential for the distinct SJ localisation of the SJ core components Mega, Kune, NrxIV and Nrg at stage 17 of embryogenesis, but not during SJ formation at stage 15. In contrast, the specific SJ localisation of Dlg, which is required for the proper SJ core complex localisation (Oshima and Fehon, 2011), is not affected by *bark*. The
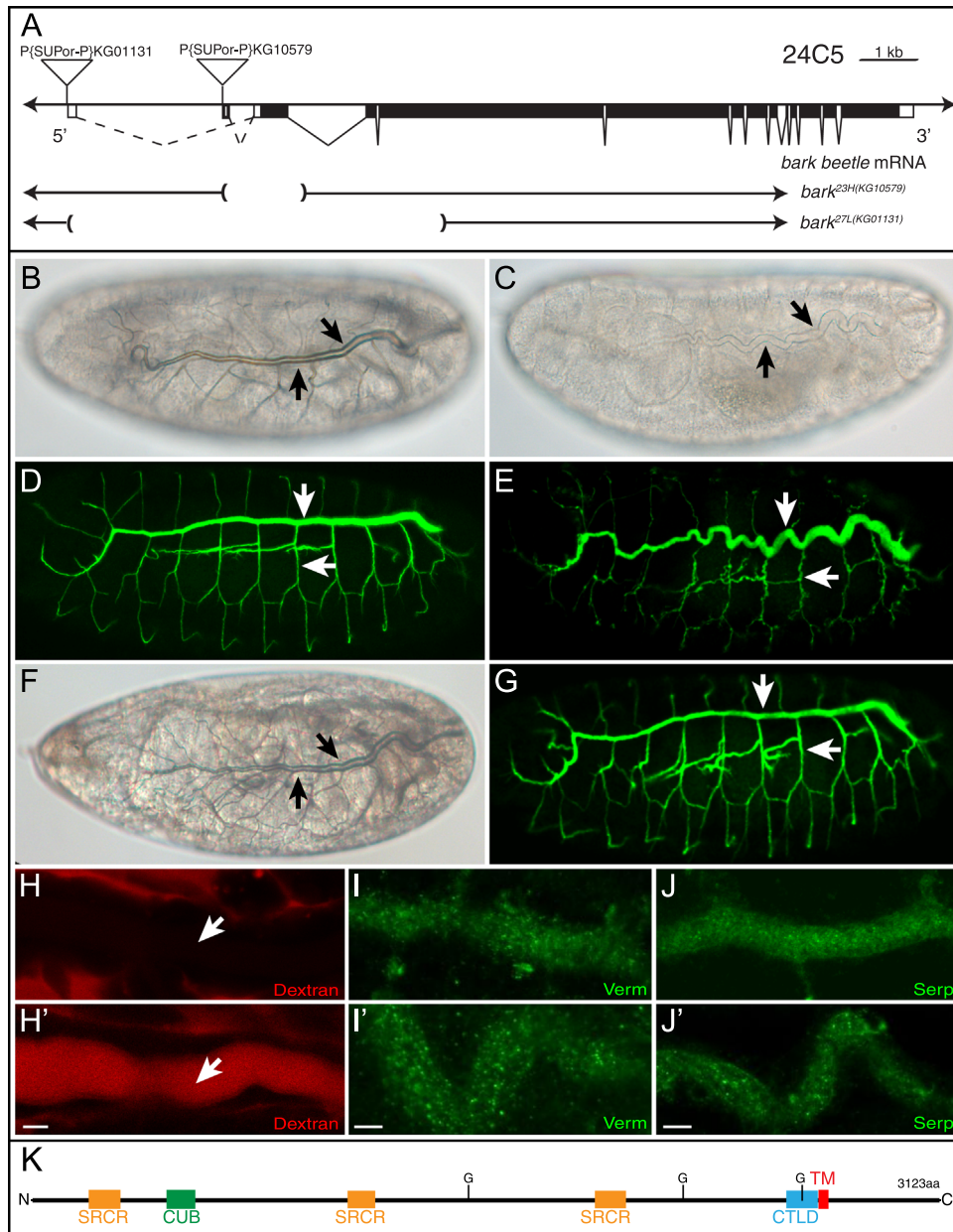
Fig. 1. Genetic and functional analysis of *bark beetle*. (A) Physical map of the genomic region 24C5 containing the *bark* gene (*CG3921*) according to FlyBase (Pierre et al., 2013). The P-elements of the enhancer trap lines P{SUPor-P}KG10579 and P{SUPor-P}KG01131 were used for P-element jump-out experiments (see Materials and methods). The genomic deletions of the *bark* alleles *bark*[23H(KG10579)] (*bark*[23H]) and *bark*[27L(KG01131)] (*bark*[27L]) are indicated. Bright field light microscopic pictures of stage 17 wild-type (B) and *bark*[23H]/Df(2L)BSC171 mutant (C) embryos. Wild-type embryos show gas filling at the end of embryogenesis (arrows in B), while *bark* mutant embryos lack tracheal gas filling (arrows in C). Stage 17 wild-type (D) and *bark*[23H]/Df(2L)BSC171 mutant (E) embryos were stained with FITC labelled chitin binding protein (CBP). CBP binds the luminal chitin matrix during tracheal development and outlines the tracheal network during embryogenesis. Wild-type embryos show straight tracheal branches (arrows in D) while *bark* mutant embryos reveal convoluted tracheal branches (arrows in E). Bright field light microscopic picture (F) and staining with FITC labelled CBP (G) of *bark*[23H], *btl*-Gal4/ *bark*[23H], UAS-*bark* mutant embryos. *bark* mutant embryos that express *bark* in tracheal cells show normal gas filling of the tracheal tubes (arrows in F) and straight tracheal branches (arrows in G) as found in wild-type embryos (compare with B, D). Confocal images of tracheal dorsal trunk branches of wild-type (H) and *bark*[23H]/Df(2L)BSC171 (H') stage 17 mutant embryos after rhodamine-dextran injection into the haemocoel. Rhodamine-dextran is not found in the dorsal trunk lumen of wild-type embryos (arrow in H), but is detectable in the dorsal trunk lumen of *bark* mutant embryos (arrow in H'). Stage 16 wild-type (I, J) and *bark*[23H]/Df(2L)BSC171 mutant (I', J') embryos were stained with anti-Verm (I, I', green) or anti-Serp (J, J', green) antibodies. The exocytosis of Serp and Verm into the tracheal lumen of *bark* mutant embryos is indistinguishable from wild-type embryos (compare I with I' and J with J'). Bars correspond to 5 μm. (K) Domain organisation of the Bark protein. The transmembrane domain (TM, red), the C-type lectin-like domain (CTLD, blue), the scavenger receptor cysteine-rich domains (SRCR, orange) the C1r/C1s; Uegf; Bmp1 domain (CUB, green) and glycosylation sites (G) are shown (Apweiler et al., 2014).

Bark localisation itself in the SJ region seems to be independent of SJ formation since Bark expression and localisation is wild-type like in *kune*, *mega* and *NrxIV* mutant embryos, which disrupt SJ development (Supplementary Fig. 3).

The co-localisation of Bark with the adherens junction marker E-cadherin, prompted us to analyse E-cadherin marker expression in *bark* mutant embryos. E-cadherin localisation resembles wild-type

during stage 15 and 17 in *bark* mutant embryos (Fig. 3F). This suggests normal adherens junction development in *bark* mutant embryos. Moreover, the apical marker Crb and phosphotyrosine are normally localised in *bark* mutant embryos during stage 15 and 17 (Fig. 3G, H), indicating wild-type like cell polarity in *bark* mutant embryos.

In summary, the combined marker gene expression analysis in *bark* mutant embryos shows normal localisation of SJ components
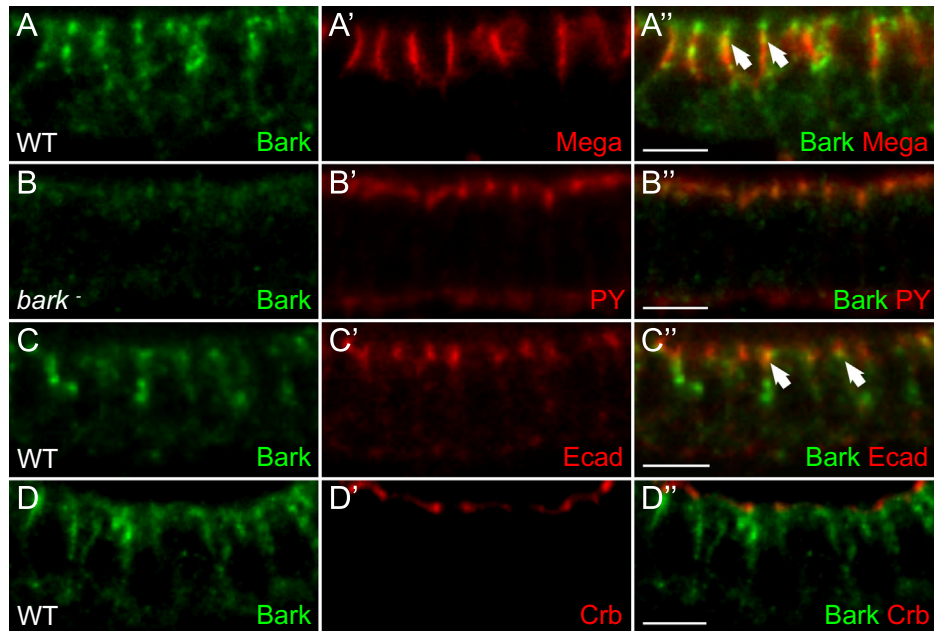
Fig. 2. Bark beetle is localised at the lateral cell membrane of hindgut cells. Whole-mount antibody double stainings of stage 16 wild-type (A, A', A″, C–D″) or *bark* mutant (B, B', B″) embryos with anti-Mega (A, A', A″), anti-Phosphotyrosine (PY20) (B, B', B″), anti-Ecad (C, C', C″), anti-Crb (D, D', D″) or anti-Bark (A–D″) antibodies. A, B, C, D and A', B', C', D' represent single-channels while A″, B″, C″, D″ represent merged channels of confocal images. The anti-Bark antibody is specific for Bark since no staining is detectable in hindgut cells of *bark* mutant embryos (green, B, B″), while PY20 control staining is present in these cells (red, B', B″). Merged images of Bark (green, A, C) and Mega (red, A') or Ecad (red, C') reveal overlapping staining of the proteins (arrows and yellow in A″, C″). Bars correspond to 5 μm.

during SJ formation but mis-localised SJ core components during stage 17 suggesting affected SJs in *bark* mutants in late embryogenesis.

Epithelial cell adhesion and septate junction formation is affected in bark beetle mutant embryos during late embryogenesis

The elongated tracheal branches, the affected transepithelial barrier and the mis-localisation of SJ core complex proteins in *bark* mutant embryos suggest that SJ morphogenesis may also be affected in *bark* mutants. To test this assumption, we analysed the ultra-structural morphology of SJs using transmission electron microscopy at stage 15 (Fig. 4A–H), stage 16 (Fig. 4I–P) and stage 17 (Fig. 4Q–Z).

During the early phase of SJ formation the trachea has not yet developed teanidial folds, which serve as an unambigous marker for the tracheal epithelium. In order to identify tracheal cells at stage 15 we took advantage of chitin fibril formation in the tracheal lumen during that stage. The chitin matrix provides a physical scaffold to shape the tracheal tubes and persists in the lumen until its degradation shortly before gas filling of the system at the end of embryogenesis (Luschnig and Uv, 2014). Thus, we stained embryo sections at stage 15 with gold-labelled wheat germ agglutinin (WGA), which labels chitin (Moussian et al., 2005), and identified the tracheal lumen by chitin detection in wild-type (Fig. 4A and B) and *bark* mutant (Fig. 4C and D) embryos. Detailed analysis of the tracheal epithelium revealed scattered septae formation in both wild-type (arrows in Fig. 4B) and *bark* mutant SJs (arrows in Fig. 4D) at stage 15. Furthermore, morphogenesis of the epidermis and septae formation of SJs in epidermal cells is similar in wild-type (Fig. 4E and F) and *bark* mutant (Fig. 4G and H) embryos.

During stage 16 wild-type embryos develop the first septae, which are characterised by the appearance of electron-dense material, in tracheal (Fig. 4I and J) and epidermal tissue (Fig. 4M and N). We observe small groups of ladder-like septae in both tissues (arrows in Fig. 4N and J). The formation of SJs is very similar in *bark* mutant embryos (Fig. 4K, L, O and P). *bark* embryos also reveal electron-dense ladder-like SJs (arrows in L and P), which are most prominent

in epidermal tissue (arrows in Fig. 4P). Occasionally small bubble-like structures are found in the region of *bark* mutant epidermal SJs (arrow in Fig. 4O). However, these bubble-like structures are smaller and more rare than found in *bark* mutants during stage 17 (see below).

Stage 17 wild-type embryos show the typical ladder-like appearance of the SJs in tracheal (Fig. 4Q, R) and epidermal cells (Fig. 4V, W). In contrast, *bark* mutant embryos have only rudimentary SJs in the trachea (Fig. 4S, U) and the epidermis (Fig. 4X, Z). Characteristic for these rudimentary SJs is the absence of the ladder-like structure in the region where normally SJs are found. Instead, only short regions of electron-dense material resembling sporadic ladder-like organisation were detected in *bark* mutant embryos (arrows in Fig. 4T, Y). Furthermore, the cell membranes of neighbouring cells detach in the putative region of SJ and form bubble-like structures between the tracheal (asterisks in Fig. 4S, U) and epidermal (asterisks in Fig. 4X, Z) cells. It is important to note that the SJ phenotypes of *bark* and SJ mutants such as *mega* or *sinu* are different. Such mutants show universal defects of the continuous ladder-like SJs (Behr et al., 2003; Wu et al., 2004), whereas *bark* mutant embryos develop short regions of wild-type like SJ organisation (arrow in Fig. 4T) flanked by regions that lack any electron-dense material where normally SJs are found (arrowheads in Fig. 4T). In contrast, adherens junction organisation in *bark* mutant embryos is wild-type like in the epidermis and the tracheal system (Supplementary Fig. 4), indicating that adherens junction formation is independent of *bark*.

In summary, *bark* mutant embryos develop SJs similar to wild-type embryos during stage 15 and 16, but develop subsequently a novel SJ phenotype in combination with cell adhesion defects.

To provide further evidence for normal establishment of SJs in *bark* mutants we analysed the time course of tracheal dorsal trunk elongation in wild-type and mutant embryos. The disruption of SJs causes an elongation of the tracheal dorsal trunk branches as found in *mega* mutant embryos (Beitel and Krasnow, 2000; Behr et al., 2003). Dorsal trunk elongation starts during early stage 16 and persists during late stage 16 and stage 17 in such embryos. In contrast, *bark* mutant embryos reveal normal dorsal trunk length
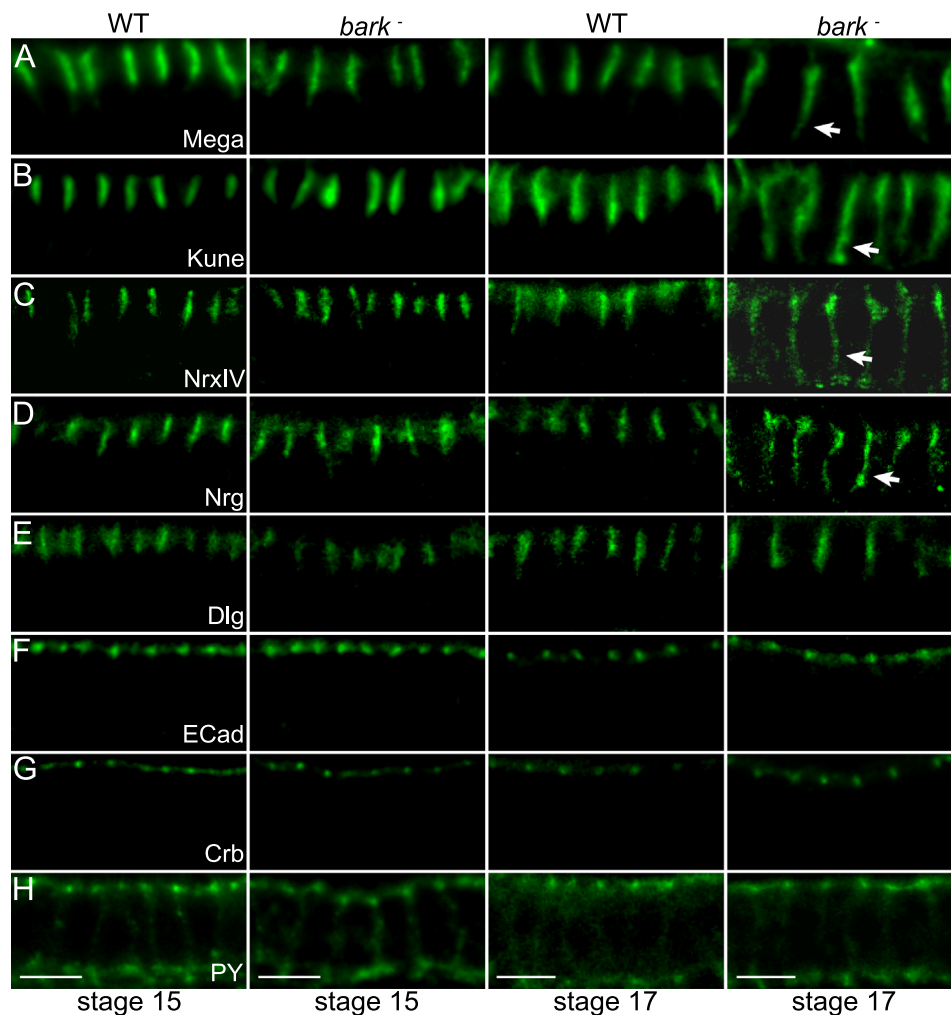
Fig. 3. SJ core components are mis-localised in hindgut cells of *bark* mutant embryos. Whole-mount antibody stainings of wild-type (WT, columns 1 and 3) or *bark*[23H]/Df(2L) BSC171 mutant (*bark*-, columns 2 and 4) embryos at stage 15 (columns 1 and 2) or stage 17 (column 3 and 4) using anti–Mega (A), anti-Kune (B), anti-Dlg (E), anti-Ecad (F), anti-Crb (G), or anti-Phosphotyrosine (PY) (H) antibodies. Whole-mount antibody stainings of NrxIV-GFP (C) or Nrg-GFP (D) (WT, columns 1 and 3) and *bark*[23H]/*bark*[23H]; NrxIV-GFP mutant (C) (*bark*-, columns 2 and 4) or Nrg-GFP; *bark*[23H]/*bark*[23H] (D) (*bark*-, columns 2 and 4) using anti-GFP antibodies. The SJ core components Mega (A), Kune (B), NrxIV (C) and Nrg (D) are mis-localised along the basolateral membrane of hindgut cells during stage 17 (arrows in A, B, C, D column 4). Bars correspond to 5 μm.

during early stage 16. Dorsal trunk length increase starts during late stage 16 and is most prominent during stage 17 (Supplementary Fig. 5). Thus, dorsal trunk increase is about 2 h delayed in *bark* mutant embryos as compared to the bona fide SJ mutant *mega*. Again these results suggest normal epithelial development in *bark* mutant embryos until early stage 16 followed by disrupted epithelial layers most prominent during stage 17.

The septate junction core complex is not disrupted in bark beetle mutant embryos

SJs are composed of single, highly ordered protein clusters called the SJ core complexes. Fluorescence recovery after photobleaching (FRAP) analysis of GFP-tagged SJ components showed low mobility of the core complex at the plasma membrane. In contrast, the GFP-tagged core proteins recovered much faster in mutants of SJ components, suggesting a disruption of the SJ core complex in such mutant embryos (Oshima and Fehon, 2011). To analyse SJ core complex stability in *bark* mutant embryos we performed corresponding FRAP analysis using the GFP-tagged SJ core complex proteins NrxIV, Nrg and ATPα. The GFP lines are homozygous viable and the GFP fusion proteins localise at the apico-lateral membrane region in the same manner as the wild-type proteins (Oshima and Fehon, 2011).

To examine the mobility of GFP-tagged proteins we performed FRAP analysis in lateral epidermal cells of wild-type and *bark* mutant embryos (Fig. 5, Supplementary Fig. 6). GFP-tagged Nrg (Fig. 5A) as well as GFP-tagged NrxIV (Fig. 5B) and GFP-tagged ATPα (Fig. 5C) display similar slow FRAP rates in *bark* mutant embryos as found in wild-type embryos. In contrast, mutants of SJ core components such as *vari* and *sinu* show a much faster FRAP rate (Fig. 5A, B, C; Oshima and Fehon, 2011). These results indicate that the SJ core complex is not disrupted in *bark* mutants, suggesting that Bark is not involved in the formation of the SJ core complex.

Intracellular Bark beetle trafficking is found in the recycling endosomes

In contrast to other integral SJ components, such as Mega, we surprisingly observed strong intracellular Bark distribution in a punctate pattern at and adjacent to the plasma membrane of epithelial cells. This observation prompted us to address Bark internalisation and further trafficking toward a degradation pathway or potentially recycling back to the plasma membrane.

Clathrin coated vesicles (CCVs) mediate internalisation of transmembrane proteins (Conner and Schmid, 2003). After CCV cleavage, vesicles fuse with an acceptor compartment, such as the early endosome (EE). From the EE, internalised proteins are routed either
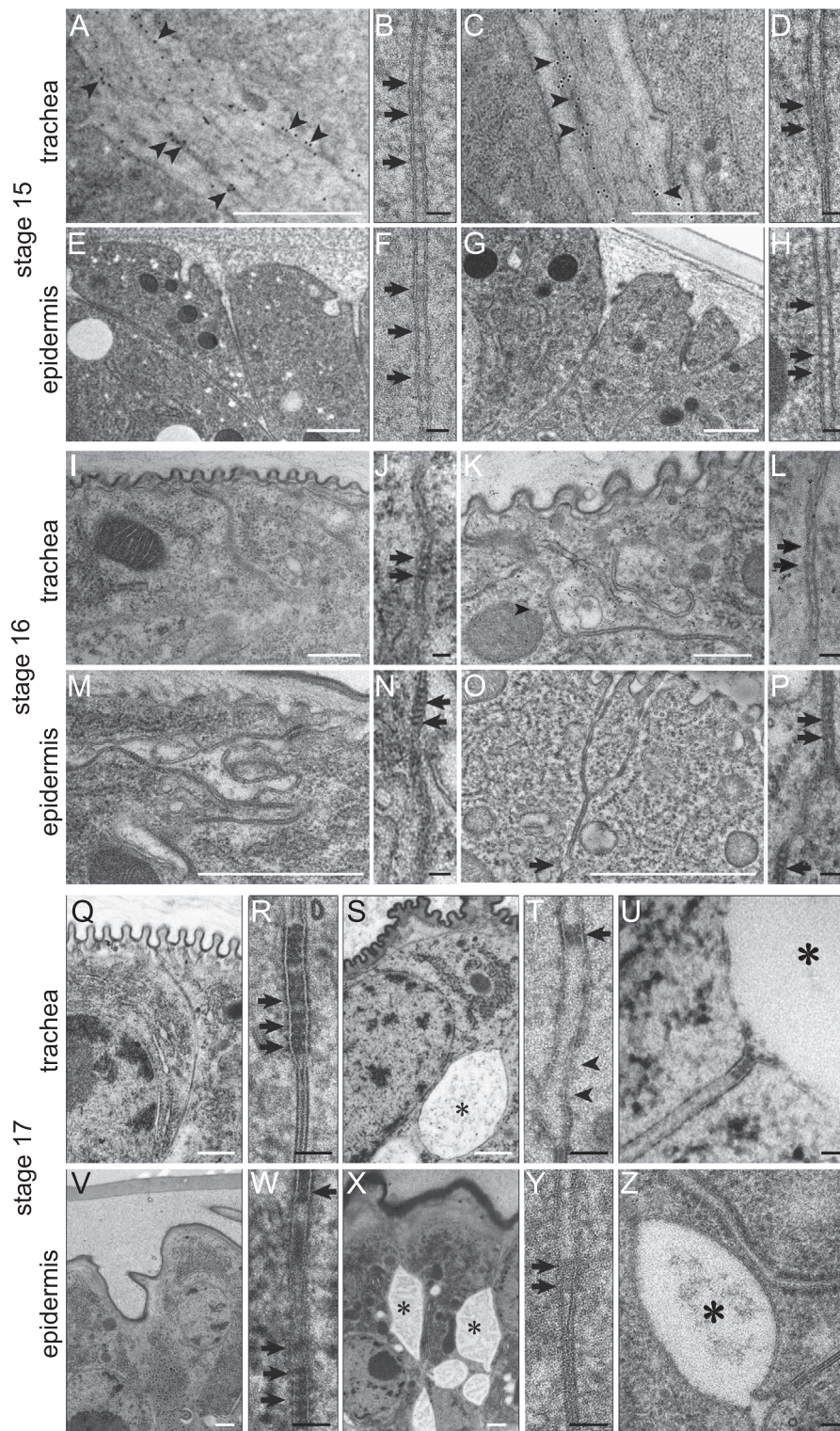
Fig. 4. *bark* mutant embryos reveal cell adhesion and SJ defects. Transmission electron microscopy of stage 15 (A–H), stage 16 (I-P) and stage 17 (Q-Z) wild-type (A,B,E,F,I,J,M, N,Q,R,V,W) and *bark* mutant (C,D,G,H,K,L,O,P,S,T,U,X,Y,Z) embryos stained with gold-labelled WGA (A–H). WGA staining (arrowheads in A and C) is indicative of chitin in the tracheal lumen (see Materials and methods). Stage 15 embryos reveal scattered septae in wild-type (arrows in B and F) and *bark* mutant (arrows in D and H) embryos. Stage 16 *bark* mutant embryos show electron-dense SJs (arrows in L and P) similar as found in wild-type embryos (arrows in J and N). Arrow in O points to a bubble–like structure in *bark* mutant epidermis. Stage 17 wild-type embryos show the typical ladder-like SJ morphology in tracheal (arrows in R) and epidermal cells (arrows in W). *bark* mutant embryos at stage 17 show only sporadic septae in tracheal (arrow in T) and epidermal (arrows in Y) cells. Large putative SJ regions lack any electron-dense material (arrowheads in T). The plasma membranes of neighbouring cells also detach in *bark* mutants and form bubble-like structures (asterisks in S,U,X,Z). Bars correspond to 500 nm (white bars) and 50 nm (black bars), respectively.

to recycling endosomes (RE) or towards the degradation pathway *via* late endosomes and lysosomes (Conner and Schmid, 2003; Mathivanan et al., 2010). We studied subcellular Bark localisation in

late stage 16 embryos, when first mutant phenotypes can be observed. Analysing epidermal cells, we found overlap of Bark with Clathrin heavy chain (Chc) (Wingen et al., 2009) (Fig. 6A″), the EE
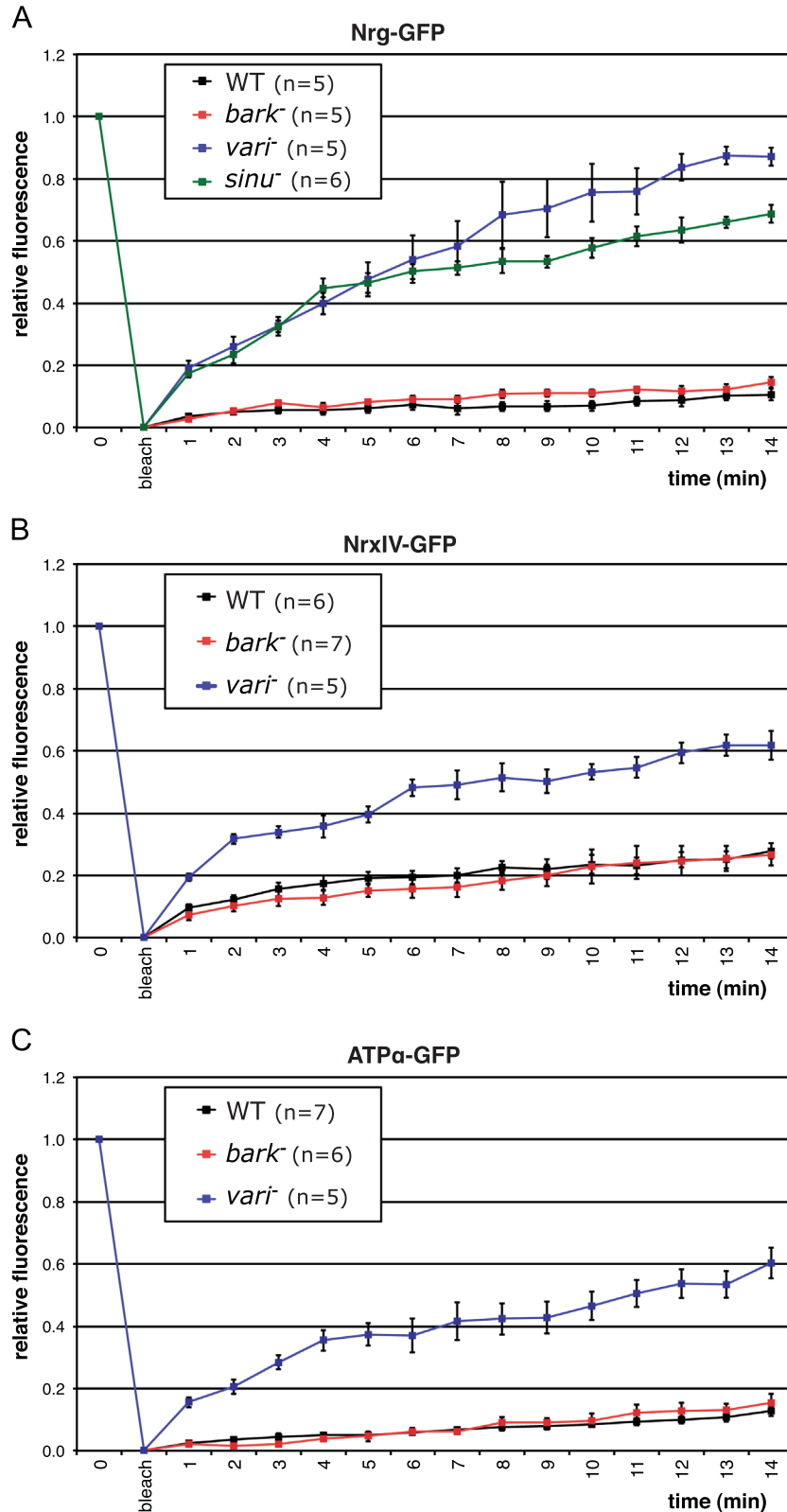
Fig. 5. SJ core proteins display wild-type like FRAP rates in *bark* mutant embryos. GFP-tagged proteins expressed in the lateral epidermis of stage 16 embryos were photobleached (see also Supplementary Fig. 2) and the average relative fluorescent recoveries of Nrg-GFP (A), NrxIV-GFP (B) and ATPα-GFP (C) in wild-type and mutant embryos were plotted. Error bars indicate standard error of the mean.

detecting Rab5 (Fig. 6B″) and the RE detecting Rab11 (Fig. 6C″; Fig. S5B). Bark was additionally found in late endosomes and lysosomes, as marked by Rab7 (Fig. 6D″; Chinchore et al., 2009) and Lamp1 (Fig. 6E″; Rusten et al., 2006). A more detailed quantitative analysis is presented in Supplementary Fig. 7. These findings indicate that clathrin mediates internalisation of Bark. Our subcellular data further provide the possibility that Bark can be sorted back to the plasma membrane *via* the recycling endosomes (Fig. 6F). Previous
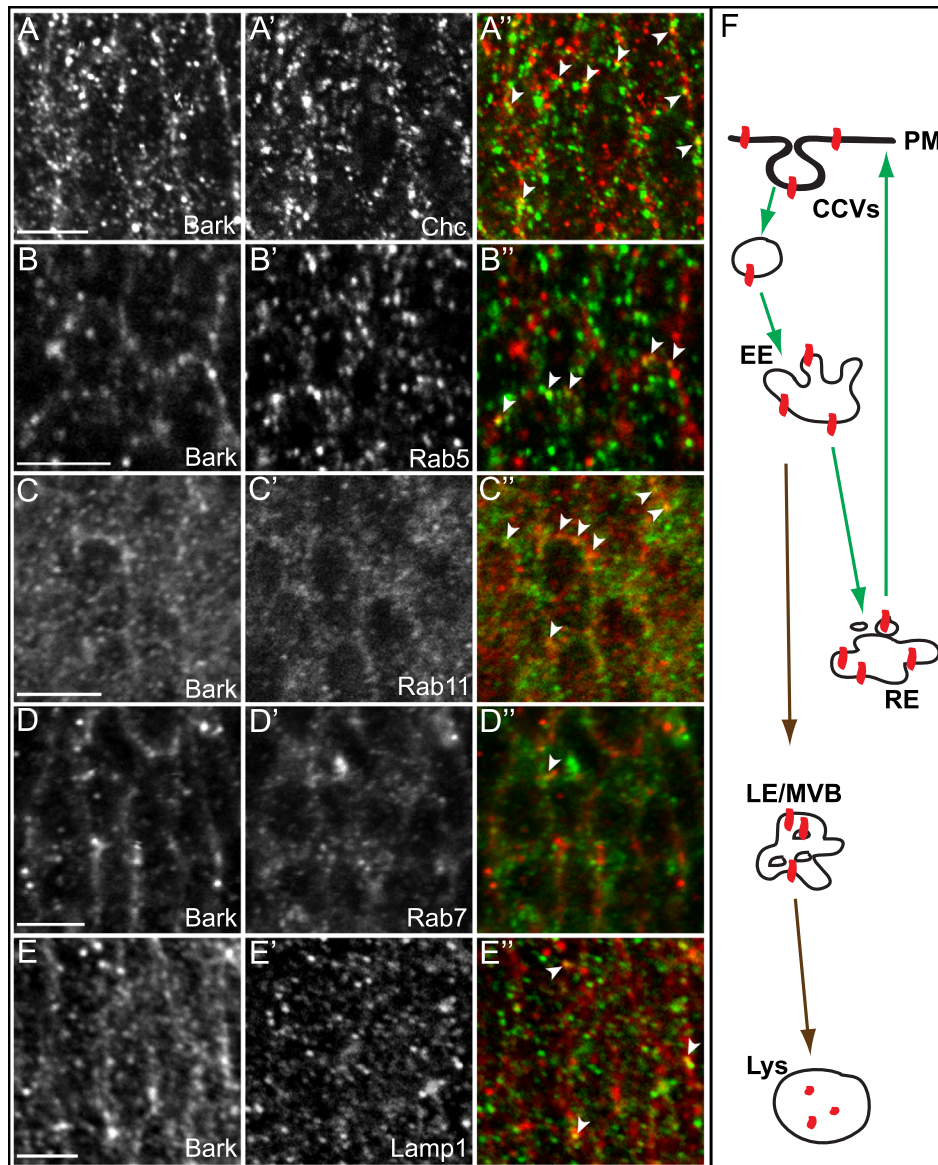
Fig. 6. Bark is localised in recycling endosomes. Whole-mount antibody double stainings of stage 16 wild-type embryos using anti-Bark (A–E) and anti-Chc (A), anti-Rab5 (B), anti-Rab11 (C), anti-Rab7 (D) or anti-Lamp1 (E) antibodies. Confocal images of epidermal cells show Bark (red) with antibodies against Clathrin heavy chain (Chc) for detecting Clathrin coated vesicles (CCVs), Rab5 for early endosomes (EE), Rab11 for recycling endosomes (RE), Rab7 for late endosomes/multi vesicular bodies (LE/MBV) and Lamp1 for lysosomes (Lys). Bark overlaps with Chc (A″), Rab5 (B″) and Rab11 (C″) as indicated by arrowheads in A″, B″ and C″ (yellow) and only occasionally with Rab7 (D″) as indicated by arrowhead in D″ (yellow). Bark that follows the degradation pathway enriches also in the lysosomes marked by Lamp1 in E″ (yellow, arrowheads). Bars correspond to 5 μm. (F) The schematic drawing illustrates how internalised Bark is routed *via* the recycling pathway (green arrows). Bark is in red.

work identified Bark as an interaction partner of the claudin Mega (Jaspers et al., 2012). Thus, we asked whether clathrin coated vesicles contain both Bark and Mega. Triple immunofluorescent stainings reveal that Bark, Mega and Chc co-localise at the cell membrane, indicating that clathrin coated vesicles localised at the cell membrane contain both Bark and Mega (Supplementary Fig. 8).

Discussion

Here we describe the characterisation and functional analysis of the putative scavenger receptor protein Bark during epithelial morphogenesis. We found that Bark is required for the maturation but not the establishment of SJs. Furthermore, Bark is involved in epithelial cell adhesion during SJ maturation.

The initiation and establishment of SJ formation appear to be independent of *bark* activity. This conclusion is based on the

observation that the ultrastructural analysis of developing wild-type and *bark* mutant SJs is similar during stage 15 and 16. At stage 15, single septae have already formed in tracheal and epithelial cells of wild-type and *bark* mutant embryos, even though the typical ladder-like septae structure of later stages is not yet established. At stage 16 electron-dense material appears in SJs of *bark* mutant embryos as found in wild-type embryos. Thus, the ultrastructural analysis suggests a normal formation of SJs in *bark* mutants until stage 16. In addition, integral SJ components are also normally localised in *bark* mutants at stage 15 suggesting correct assembly of the SJs. Furthermore, the exocytosis of Serpentine and Vermiform into the tracheal lumen mediated by SJs during stage 16 (Luschnig et al., 2006; Wang et al., 2006) is not affected in *bark* mutants, suggesting normal SJ function independent of *bark*. Remarkable is the delay of tracheal dorsal trunk elongation in *bark* mutants. Embryos in which the initial SJ formation is affected as found in *mega* (Behr et al., 2003) display dorsal trunk elongation about two

hours earlier than observed in *bark* mutants. Thus, establishment of SJs seems to be normal in *bark* mutants, since dorsal trunk elongation is indicative for disrupted SJs (Wu and Beitel, 2004). Taken together, these results suggest that Bark does not critically participate in the initial morphogenesis and functional properties of SJs.

In contrast, subsequent SJ maturation (stage 17) strongly depends on Bark. Rhodamine-dextran injection experiments revealed that the transepithelial barrier function of SJs is compromised in *bark* mutants. In such embryos the wild-type ladder-like SJ structure is disrupted, only rudimentary septae are formed and cell adhesion is impaired. This phenotype is distinct from the archetypal SJ phenotype observed in mutants of the SJ core complexes, e.g. in *mega* or *Nrg* mutant embryos. In these mutants the septae are either reduced in number or are absent, while cell adhesion seems not to be affected, i.e. the uniform spacing between the plasma membranes of adjacent epithelial cells is maintained (Behr et al., 2003; Genova and Fehon, 2003). Individual *bark* mutant embryos develop a great diversity of septae ranging from no detectable septae in places where septae would normally form to rudimentary septae and up to wild-type like septae. Furthermore, such mutant embryos show an erratic spacing of the epithelial plasma membranes; in extreme cases the plasma membranes detach from each other resulting in gaps between the cells. Such cell adhesion defects of *bark* epithelial cells have also been observed in mutants of Gliotactin, a marker for tricellular junctions (Schulte et al., 2003), but so far in no other mutant that affects SJs.

The phenotypic differences between *bark* and archetypal SJ lack-of-function mutant embryos are also observed in gain-of-function experiments. Overexpression of Bark does not interfere with normal development or the barrier function of SJs and rescues the *bark* mutant phenotype. In contrast, overexpression of other SJ components causes mis-localisation of the components and a disruption of the barrier function. Thus, it has been proposed that SJ components are functionally interdependent (Behr et al., 2003; Genova and Fehon, 2003). Our observation that the level of Bark is not critical for *bark* function supports the argument that *bark* mediates a distinct role during SJ maturation in late embryogenesis.

The detachment of lateral cell membranes, which occasionally deteriorate and form gaps between the epithelial cells of *bark* mutant embryos, indicates that Bark plays also a role in epithelial cell adhesion in addition to its function in SJ integrity. As Bark represents a large transmembrane protein, it may mediate the cell–cell adhesion through homophilic interactions. We tested this possibility and analysed putative homophilic Bark binding in a cell aggregation assay, but could not detect any homophilic Bark binding (unpublished results). However, we cannot exclude homophilic binding in the embryo, since posttranslational modifications may not occur in the cell culture system. Such modifications could include the attachment of sugar moieties *via* several potential glycosylation sites noted in the extracellular Bark domain and/or binding of sugar moieties to Bark *via* its lectin domain (Baycin-Hizal et al., 2011). Heterophilic Bark binding with an already identified SJ component is also not very likely, since the lack of such components has no effect on cell adhesion in the region of SJs. Thus, we speculate that Bark mediates its cell adhesion function by homophilic binding, which depends on specific posttranslational modifications, or in conjunction with an unknown interaction partner.

The distinctive feature of SJs is that they must maintain their functional properties, in particular the control of the transepithelial barrier function, while cells rearrange during tissue morphogenesis. Thus, epithelial layers must be able to simultaneously alter cell–cell-contacts, shuffle SJ protein components and establish functional SJ structures, which create distinct fluid compartments (Fristrom, 1982). Given these features, the questions that come to mind are: What is the molecular basis of these distinct requirements and what is the role of Bark?

The recent finding of a stable SJ multiprotein core complex is an important step in understanding SJ protein dynamics. The SJ core complex is preassembled intracellularly before its incorporation into the SJs at the plasma membrane. Interestingly, the core complex seems to be stable even in cells actively rearranging their contacts (Oshima and Fehon, 2011). Our FRAP experiments indicate that the core complex is also stable in *bark* mutants, but the morphology and function of SJs are severely affected. The mis-localisation of SJ core components along the basolateral cell membrane in stage 17 *bark* mutants suggest that the SJ core complexes do not properly coalesce to assemble SJs in the apicolateral membrane region. This observation is consistent with previous binding studies suggesting a direct interaction of Bark with Mega or another SJ core protein (Jaspers et al., 2012). Thus, we speculate that Bark provides a scaffold-like matrix serving as a platform for the SJ core complexes, which assemble into functional SJs. The potential Bark matrix is not necessary for establishment of SJs, but becomes essential during tissue morphogenesis, i.e. during SJ maturation to ensure that SJ core complexes remain well-ordered and able to sustain the epithelial barrier function. This role of Bark becomes particularly apparent during morphogenesis of the embryonic tracheal system, which is established by extensive cell shape changes and cell–cell rearrangements. Such a possible role would explain why a lack of Bark leads not only to cell adhesion defects and SJ failure, but also to a severely mis-shapen, convoluted tracheal system.

A scenario that would then allow for cell–cell rearrangement is that Bark is regulated in a way that it may detach from defined regions within the SJs and thereby reduce both cell adhesion and SJ integrity, which results in SJ core complex release. Such opened SJ sub-regions may in turn tolerate cell–cell rearrangements, while nearby sub-regions may still contain functional septae that establish the transepithelial barrier function. Consistent with this view is our observation that Bark localises to recycling endosomes within intracellular compartments. Thus, Bark may shuttle from sites of SJ breakdown to sites of SJ assembly *via* the recycling endosomal pathway. At the site of SJ assembly Bark might mediate dual functions in cell adhesion and providing anchor points for the SJ core complexes.

Acknowledgements

Appendix A. Supporting information

Supplementary data associated with this article can be found in the online version at http://dx.doi.org/10.1016/j.ydbio.2015.02.008.

References

Angelow, S., Ahlstrom, R., Yu, A.S.L., 2008. Biology of claudins. Am. J. Physiol. Renal Physiol.. 295, F867–76. http://dx.doi.org/10.1152/ajprenal.90264.2008.
Apweiler, R., Bateman, A., Martin, M.J., O'Donovan, C., Magrane, M., Alam-Faruque, Y., Alpi, E., Antunes, R., Arganiska, J., Casanova, E.B., Bely, B., Bingley, M., Bonilla, C., Britto, R., Bursteinas, B., Chan, W.M., Chavali, G., Cibrian-Uhalte, E., Da Silva, A., De Giorgi, M., Fazzini, F., Gane, P., Castro, L.G., Garmiri, P., Hatton-Ellis, E., Hieta, R., Huntley, R., Legge, D., Liu, W., Luo, J., MacDougall, A., Mutowo, P., Nightingale, A., Orchard, S., Pichler, K., Poggioli, D., Pundir, S., Pureza, L., Qi, G., Rosanoff, S., Sawford, T., Shypitsyna, A., Turner, E., Volynkin, V., Wardell, T., Watkins, X., Zellner, H., Corbett, M., Donnelly, M., Van Rensburg, P., Goujon, M., McWilliam, H., Lopez, R., Xenarios, I., Bougueleret, L., Bridge, A., Poux, S., Redaschi, N., Aimo, L., Auchincloss, A., Axelsen, K., Bansal, P., Baratin, D., Binz, P.-A., Blatter, M.-C., Boeckmann, B., Bolleman, J., Boutet, E., Breuza, L., Casal-Casas, C., de Castro, E., Cerutti, L., Coudert, E., Cuche, B., Doche, M., Dornevil, D., Duvaud, S., Estreicher, A.,

Famiglietti, M., Feuermann, M., Gasteiger, E., Gehant, S., Gerritsen, V., Gos, A., Gruaz-Gumowski, N., Hinz, U., Hulo, C., James, J., Jungo, F., Keller, G., Lara, V., Lemercier, P., Lew, J., Lieberherr, D., Lombardot, T., Martin, X., Masson, P., Morgat, A., Neto, T., Paesano, S., Pedruzzi, I., Pilbout, S., Pozzato, M., Pruess, M., Rivoire, C., Roechert, B., Schneider, M., Sigrist, C., Sonesson, K., Staehli, S., Stutz, A., Sundaram, S., Tognolli, M., Verbregue, L., Veuthey, A.-L., Wu, C.H., Arighi, C.N., Arminski, L., Chen, C., Chen, Y., Garavelli, J.S., Huang, H., Laiho, K., McGarvey, P., Natale, D.A., Suzek, B.E., Vinayaka, C.R., Wang, Q., Wang, Y., Yeh, L.-S., Yerramalla, M.S., Zhang, J., Consortium, U., 2014. Activities at the Universal Protein Resource (UniProt). Nucleic Acids Res. 42, D191–D198. http://dx.doi.org/10.1093/nar/gkt1140.

Baumgartner, S., Littleton, J.T., Broadie, K., Bhat, M.A., Harbecke, R., Lengyel, J.A., Chiquet-Ehrismann, R., Prokop, A., Bellen, H.J., 1996. A Drosophila neurexin is required for septate junction and blood-nerve barrier formation and function. Cell 87, 1059–1068.

Baycin-Hizal, D., Tian, Y., Akan, I., Jacobson, E., Clark, D., Chu, J., Palter, K., Zhang, H., Betenbaugh, M.J., 2011. GlycoFly: a database of Drosophila N-linked glycoproteins identified using SPEG−MS techniques. J. Proteome Res. 10, 2777–2784. http://dx.doi.org/10.1021/pr200004t.

Behr, M., Riedel, D., Schuh, R., 2003. The claudin-like Megatrachea is essential in septate junctions for the epithelial barrier function in Drosophila. Dev. Cell 5, 611–620.

Beitel, G.J., Krasnow, M.A., 2000. Genetic control of epithelial tube size in the Drosophila tracheal system. Development 127, 3271–3282.

Brand, A.H., Perrimon, N., 1993. Targeted gene expression as a means of altering cell fates and generating dominant phenotypes. Development 118, 401–415.

Chinchore, Y., Mitra, A., Dolph, P.J., 2009. Accumulation of rhodopsin in late endosomes triggers photoreceptor cell degeneration. PLoS Genet 5, e1000377. http://dx.doi.org/10.1371/journal.pgen.1000377.

Conner, S.D., Schmid, S.L., 2003. Regulated portals of entry into the cell. Nature 422, 37–44. http://dx.doi.org/10.1038/nature01451.

Fehon, R.G., Dawson, I.A., Artavanis-Tsakonas, S., 1994. A Drosophila homologue of membrane-skeleton protein 4.1 is associated with septate junctions and is encoded by the coracle gene. Development 120, 545–557.

Fristrom, D.K., 1982. Septate junctions in imaginal disks of Drosophila: a model for the redistribution of septa during cell rearrangement. J. Cell Biol. 94, 77–87.

Furuse, M., Tsukita, S., 2006. Claudins in occluding junctions of humans and flies. Trends Cell Biol. 16, 181–188. http://dx.doi.org/10.1016/j.tcb.2006.02.006.

Genova, J.L., Fehon, R.G., 2003. Neuroglian, Gliotactin, and the Na+/K+ ATPase are essential for septate junction function in Drosophila. J. Cell Biol. 161, 979–989. http://dx.doi.org/10.1083/jcb.200212054.

Hartenstein, V., Jan, Y.N., 1992. Studying Drosophila embryogenesis with P-Lacz enhancer trap lines. Roux. Arch. Dev. Biol. 201, 194–220.

Jaspers, M.H.J., Nolde, K., Behr, M., Joo, S.-H., Plessmann, U., Nikolov, M., Urlaub, H., Schuh, R., 2012. The claudin Megatrachea protein complex. J. Biol. Chem. 287, 36756–36765. http://dx.doi.org/10.1074/jbc.M112.399410.

Knust, E., Bossinger, O., 2002. Composition and formation of intercellular junctions in epithelial cells. Science 298, 1955–1959. http://dx.doi.org/10.1126/science.1072161.

Lal-Nag, M., Morin, P.J., 2009. The claudins. Genome Biol. 10, 235. http://dx.doi.org/10.1186/gb-2009-10-8-235.

Lamb, R.S., Ward, R.E., Schweizer, L., Fehon, R.G., 1998. Drosophila coracle, a member of the protein 4.1 superfamily, has essential structural functions in the septate junctions and developmental functions in embryonic and adult epithelial cells. Mol. Biol. Cell 9, 3505–3519.

Le, T., Liang, Z., Patel, H., Yu, M.H., Sivasubramaniam, G., Slovitt, M., Tanentzapf, G., Mohanty, N., Paul, S.M., Wu, V.M., Beitel, G.J., 2006. A new family of Drosophila balancer chromosomes with a w- dfd-GMR yellow fluorescent protein marker. Genetics 174, 2255–2257. http://dx.doi.org/10.1534/genetics.106.063461.

Luschnig, S., Bätz, T., Armbruster, K., Krasnow, M.A., 2006. serpentine and vermiform encode matrix proteins with chitin binding and deacetylation domains that limit tracheal tube length in Drosophila. Curr. Biol. 16, 186–194. http://dx.doi.org/10.1016/j.cub.2005.11.072.

Luschnig, S., Uv, A., 2014. Luminal matrices: an inside view on organ morphogenesis. Exp. Cell Res. 321, 64–70. http://dx.doi.org/10.1016/j.yexcr.2013.09.010.

Manders, E.M.M., Verbeek, F.J., Aten, J.A., 1993. Measurement of colocalization of objects in dual-color confocal images. J. Microsc.-Oxford 169, 375–382.

Mathivanan, S., Ji, H., Simpson, R.J., 2010. Exosomes: extracellular organelles important in intercellular communication. J. Proteomics 73, 1907–1920. http://dx.doi.org/10.1016/j.jprot.2010.06.006.

Moussian, B., Schwarz, H., Bartoszewski, S., Nüsslein-Volhard, C., 2005. Involvement of chitin in exoskeleton morphogenesis in Drosophila melanogaster. J. Morphol. 264, 117–130. http://dx.doi.org/10.1002/jmor.10324.

Moussian, B., Seifarth, C., Müller, U., Berger, J., Schwarz, H., 2006. Cuticle differentiation during Drosophila embryogenesis. Arthropod. Struct. Dev. 35, 137–152. http://dx.doi.org/10.1016/j.asd.2006.05.003.

Nelson, K.S., Furuse, M., Beitel, G.J., 2010. The Drosophila Claudin Kune-kune is required for septate junction organisation and tracheal tube size control. Genetics 185, 831–839. http://dx.doi.org/10.1534/genetics.110.114959.

Oda, H., Uemura, T., Harada, Y., Iwai, Y., Takeichi, M., 1994. A Drosophila homolog of cadherin associated with armadillo and essential for embryonic cell–cell adhesion. Dev. Biol. 165, 716–726. http://dx.doi.org/10.1006/dbio.1994.1287.

Oshima, K., Fehon, R.G., 2011. Analysis of protein dynamics within the septate junction reveals a highly stable core protein complex that does not include the basolateral polarity protein Discs large. J. Cell Sci. 124, 2861–2871. http://dx.doi.org/10.1242/jcs.087700.

Parnas, D., Haghighi, A.P., Fetter, R.D., Kim, S.W., Goodman, C.S., 2001. Regulation of postsynaptic structure and protein localisation by the Rho-type guanine nucleotide exchange factor dPix. Neuron 32, 415–424.

Patel, N.H., Snow, P.M., Goodman, C.S., 1987. Characterization and cloning of Fasciclin III: a glycoprotein expressed on a subset of neurons and axon pathways in Drosophila. Cell 48, 975–988. http://dx.doi.org/10.1016/0092-8674(87)90706-9.

Paul, S.M., Ternet, M., Salvaterra, P.M., Beitel, G.J., 2003. The Na+/K+ ATPase is required for septate junction function and epithelial tube-size control in the Drosophila tracheal system. Development 130, 4963–4974. http://dx.doi.org/10.1242/dev.00691.

Pierre, S.E.S., Ponting, L., Stefancsik, R., McQuilton, P., McQuilton, P., 2013. FlyBase 102–advanced approaches to interrogating FlyBase. Nucleic Acids Res. 42, D780–D788. http://dx.doi.org/10.1093/nar/gkt1092.

Rodriguez-Boulan, E., Nelson, W.J., 1989. Morphogenesis of the polarized epithelial cell phenotype. Science 245, 718–725.

Rubin, G.M.G., Spradling, A.C.A., 1982. Genetic transformation of Drosophila with transposable element vectors. Science 218, 348–353.

Rusten, T.E., Rodahl, L.M.W., Pattni, K., Englund, C., Samakovlis, C., Dove, S., Brech, A., Stenmark, H., 2006. Fab1 phosphatidylinositol 3-phosphate 5-kinase controls trafficking but not silencing of endocytosed receptors. Mol. Biol. Cell 17, 3989–4001. http://dx.doi.org/10.1091/mbc.E06-03-0239.

Satoh, A.K., O'Tousa, J.E., Ozaki, K., Ready, D.F., 2005. Rab11 mediates post-Golgi trafficking of rhodopsin to the photosensitive apical membrane of Drosophila photoreceptors. Development 132, 1487–1497. http://dx.doi.org/10.1242/dev.01704.

Schneeberger, E.E., Lynch, R.D., 1992. Structure, function, and regulation of cellular tight junctions. Am. J. Physiol. 262, L647–61.

Schulte, J., Tepass, U., Auld, V.J., 2003. Gliotactin, a novel marker of tricellular junctions, is necessary for septate junction development in Drosophila. J. Cell Biol. 161, 991–1000. http://dx.doi.org/10.1083/jcb.200303192.

Tepass, U., Tanentzapf, G., Ward, R., Fehon, R., 2001. Epithelial cell polarity and cell junctions in Drosophila. Annu. Rev. Genet. 35, 747–784. http://dx.doi.org/10.1146/annurev.genet.35.102401.091415.

Tepass, U., Theres, C., Knust, E., 1990. crumbs encodes an EGF-like protein expressed on apical membranes of Drosophila epithelial cells and required for organisation of epithelia. Cell 61, 787–799.

Tsukita, S., Furuse, M., 2002. Claudin-based barrier in simple and stratified cellular sheets. Curr. Opin. Cell Biol. 14, 531–536.

Tsukita, S., Furuse, M., Itoh, M., 2001. Multifunctional strands in tight junctions. Nat. Rev. Mol. Cell Biol. 2, 285–293. http://dx.doi.org/10.1038/35067088.

Turksen, K., Troy, T.-C., 2004. Barriers built on claudins. J. Cell Sci. 117, 2435–2447. http://dx.doi.org/10.1242/jcs.01235.

Wang, S., Jayaram, S.A., Hemphälä, J., Senti, K.-A., Tsarouhas, V., Jin, H., Samakovlis, C., 2006. Septate-junction-dependent luminal deposition of chitin deacetylases restricts tube elongation in the Drosophila trachea. Curr. Biol. 16, 180–185. http://dx.doi.org/10.1016/j.cub.2005.11.074.

Ward, R.E., Lamb, R.S., Fehon, R.G., 1998. A conserved functional domain of Drosophila Coracle is required for localisation at the septate junction and has membrane-organizing activity. J. Cell Biol. 140, 1463–1473.

Ward, R.E., Schweizer, L., Lamb, R.S., Fehon, R.G., 2001. The protein 4.1, ezrin, radixin, moesin (FERM) domain of Drosophila Coracle, a cytoplasmic component of the septate junction, provides functions essential for embryonic development and imaginal cell proliferation. Genetics 159, 219–228.

Wingen, C., Stümpges, B., Hoch, M., Behr, M., 2009. Expression and localisation of clathrin heavy chain in Drosophila melanogaster. Gene Expr. Patterns 9, 549–554. http://dx.doi.org/10.1016/j.gep.2009.06.007.

Woods, D.F., Hough, C., Peel, D., Callaini, G., Bryant, P.J., 1996. Dlg protein is required for junction structure, cell polarity, and proliferation control in Drosophila epithelia. J. Cell Biol. 134, 1469–1482.

Wu, V.M., Beitel, G.J., 2004. A junctional problem of apical proportions: epithelial tube-size control by septate junctions in the Drosophila tracheal system. Curr. Opin. Cell Biol. 16, 493–499. http://dx.doi.org/10.1016/j.ceb.2004.07.008.

Wu, V.M., Schulte, J., Hirschi, A., Tepass, U., Beitel, G.J., 2004. Sinuous is a Drosophila claudin required for septate junction organisation and epithelial tube size control. J. Cell Biol. 164, 313–323. http://dx.doi.org/10.1083/jcb.200309134.

Wu, V.M., Yu, M.H., Paik, R., Banerjee, S., Liang, Z., Paul, S.M., Bhat, M.A., Beitel, G.J., 2007. Drosophila Varicose, a member of a new subgroup of basolateral MAGUKs, is required for septate junctions and tracheal morphogenesis. Development 134, 999–1009. http://dx.doi.org/10.1242/dev.02785.

Wucherpfennig, T., Wilsch-Bräuninger, M., González-Gaitán, M., 2003. Role of Drosophila Rab5 during endosomal trafficking at the synapse and evoked neurotransmitter release. J. Cell Biol. 161, 609–624. http://dx.doi.org/10.1083/jcb.200211087.